Sub-10 nm lithography with self-assembled monolayers

M. J. Lercel and H. G. Craighead
School of Engineering and Applied Physics, Cornell University, Ithaca, New York 14853

A. N. Parikh, K. Seshadri, and D. L. Allara
Department of Materials Science and Department of Chemistry, Pennsylvania State University, University Park, Pennsylvania 16802

(Received 9 October 1995; accepted for publication 4 January 1996)

Dots demonstrating critical resist dimensions of approximately 5 to 6 nm were formed in an octadecylsiloxane monolayer on silicon by electron beam exposure using a digital scanning electron microscope at 20 keV beam energy. The patterned dots were observed by imaging with an atomic force microscope (AFM). The electron beam size was measured to confirm that it is not the limiting factor in the exposure resolution. The limit that prevents the observation of smaller structures is either the small contrast in the AFM imaging for smaller dots or an intrinsic material limit caused by the secondary electron range. © *1996 American Institute of Physics.* [S0003-6951(96)01011-0]

The production of sub-10 nm structures in electron beam resists is difficult.[1] It has been achieved with poly(methyl methacrylate) (PMMA) resists exposed at 100 keV beam energy[2,3] and with inorganic resists at similar beam voltages.[4] For high resolution with PMMA, the development step is critical and production of sub-10 nm lines require an increase in exposure dose.[3] Although inorganic resists are capable of even smaller critical dimensions, they require high electron doses at high beam energies because this exposure mechanism involves only primary electron damage.

An ideal high-resolution electron beam resist also needs to be thin to avoid forward scattering of the primary beam. Further, a very thin resist allows a lower primary beam energy to be used that increases the resist sensitivity through more efficient energy deposition in the resist layer. Lower beam energy also reduces electron backscattering that tends to reduce resist exposure contrast. Because of these factors, it is useful to explore the resolution at low beam energies.

Self-assembled monolayers (SAMs) are very thin organic layers that are formed by the attachment of single organic chains in an ordered arrangement to a variety of surfaces by chemical bonding. The size of the molecule determines the layer thickness and can be carefully controlled to produce layers of uniform coverage typically ~1–3 nm thick.[5] These materials are candidates for very high resolution resists not only because they are very thin but also the important lateral dimension of the films is a molecular diameter (<1 nm for these materials). Previously, we have demonstrated high-resolution patterning (<25 nm) of these materials with focused electron beams and scanned probe modifications and subsequent use of the layers as masks for wet or plasma chemical etching.[6–8] In this letter, we demonstrate sub-10 nm patterning of these materials and compare this to the competing effect of contamination lithography. Since the patterning dimensions are approaching the possible material limits, the exposing electron beam size is also measured independently to see if the critical dimensions are limited by the beam size.

The SAMs of octadecylsiloxanes (ODS) were grown on the native oxide on Si (100) wafers in a solution of octadecyltrichlorosilane (1 mM solution for 30 min) in hexadecane and chloroform in a standard process as used in our previous studies.[6–8] The surfaces of the ODS films were confirmed to have very small surface roughness (<0.15 nm RMS[9]) through atomic force microscopy (AFM) inspection.

The AFM was used in contact mode, friction force mode (FFM), and Tapping Mode™ (TM-)[10] to image the films after electron beam exposure. Since the resulting topographical change in the films is very small, the torsional effects on the cantilevers caused by the higher friction in the exposed regions dominates the contact mode imaging.[11] The exposed regions are known from wetting measurements to have a higher surface energy than the as-formed film,[8] and this should correspond to a higher friction for the AFM tip.

The ODS layers were modified by a Zeiss DSM 982 scanning electron microscope (SEM) with a chamber vacuum $\sim 10^{-6}$ Torr. The digital rastering of the beam in slow scan modes consists of an array dot exposures. The dots are slightly elongated in the scan direction because of beam settling time, so dimensions transverse to the raster direction are used for resist resolution measurements. Exposures usually consisted of an entire slow scan frame at about 200 μm field size using a pixel density of 512×480. The array pitch could be modified by changing the frame size or the pixel density, but all exposures were carried out at large enough pitches so that there was no overlap between exposed dots. The slow scan speed (time per frame) and the beam current were varied to obtain different doses. A short working distance of ~4–5 mm was used to minimize the effects of stray electromagnetic fields.

The SEM beam size was measured both by examining the secondary electron (SE) resolution and doing a transmitted current measurement across a cleaved wafer edge. The transmitted electron (TE) current was measured by scanning over a cleaved Si or GaAs edge suspended over a screw hole and measuring the stage current.[12] All readings were taken at time spacings (100–250 ms) significantly slower than the picoammeter rise time.[13] An attempt was made to tilt the sample to align the wafer edge parallel to the beam; however, this did not provide better results over searching the cleaved edge for a sharp drop-off. The TE measurements were fitted to a Gaussian or hyperbolic tangent profile and the beam width was estimated from the fit parameters. The functional profile was chosen for convenience in estimating the critical points of the beam profile. For the tanh fit, $\mathrm{TE}(x) = a + b \tanh[(x-d)/c]$, the separation between the 75% and 25%

0003-6951/96/68(11)/1504/3/$10.00
© 1996 American Institute of Physics
Downloaded¬25¬Mar¬2006¬to¬169.237.215.179.¬Redistribution¬subject¬to¬AIP¬license¬or¬copyright,¬see¬http://apl.aip.org/apl/copyright.jsp

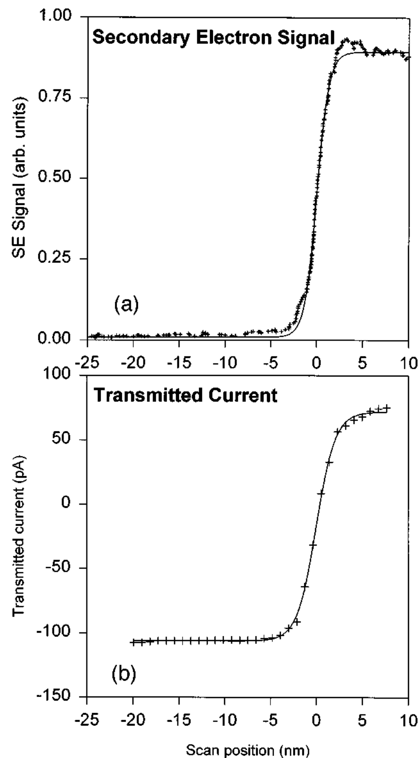

FIG. 1. (a) Secondary electron signal measured in the SEM when the beam is scanned over a cleaved GaAs wafer edge with curve fit that indicates the electron beam has a Gaussian full width of 1.98 nm. (b) Transmitted electron signal from the same scan and fit that indicates a Gaussian full width of 3.1 nm.

points on the TE signal is ~0.7*c*, see Fig. 1(b). This corresponds to a full Gaussian beam width of ~1.48*c*.[12] At 20 keV, the beam size estimated from the transmitted current was ~3.1 nm. The SE profile over the step edge, measured simultaneously with the TE signal, shows a sharper edge than the transmitted current. This is due to the large beam penetration at 20 keV through the thin exposed wafer edge. Under similar conditions, the SE linescan, Fig. 1(a), predicts a beam size of ~1.98 nm (compared to 3.1 nm for the TE linescan). At 1 keV, the TE profile shows that the center portion of the beam had a Gaussian width of ~9 nm, but a longer tail (with Gaussian width of ~20 nm) extended farther from the step edge. This tail was also observed in the SE linescan across the step edge.

Since this SEM is not equipped with a sample transfer chamber and the chamber vacuum is not as clean, the issue of contamination writing versus electron beam damage of the ODS layer becomes more critical. Contamination was observed at higher doses and could be separated from the resist exposures. In scanning with the AFM, the exposed monolayer areas appeared slightly lower (~0.35 to 0.55 nm, lower is darker in the AFM gray scale) than the unexposed film, and the contamination appeared as a raised structure (often more than 8 nm high and increasing with dose). Figure 2 shows an image with both monolayer exposure (lowered areas) and contamination lithography (raised areas). A control wafer with no monolayer showed only the raised contamination structures without the lowered areas around them. It is useful to note that for a 400 fC/dot exposure, the width of the dark ring in the AFM image was about 430 nm, which is an

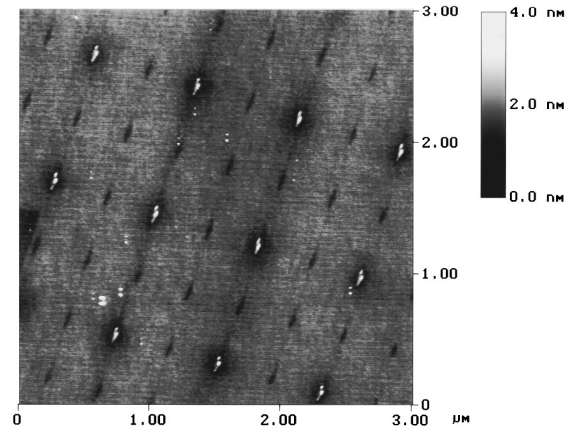

FIG. 2. AFM image of monolayer exposure (dark area) and contamination exposure (light area) for an exposure at 20 keV electron energy and dose of ~8.8 fC/dot (finer pitch) and ~91 fC/dot (larger pitch).

area dose of ~275 $\mu C/cm^2$, but the contamination dot was about 72 nm across for an area dose of ~9.8 mC/cm^2. The lower dose is very similar to what we have reported earlier for the critical dose for monolayer exposure.[6] TMAFM imaging showed very little height difference in the exposed areas, but clearly showed the raised areas from contamination writing. Since the monolayer is more sensitive to exposure than contamination lithography, the lowered exposed monolayer areas are always larger than the contamination dots. No contamination was observed at doses less than ~22 fc/dot at 20 keV. Above this threshold, contamination dots of ~6 nm across were produced on an ODS-covered Si wafer at a dose of ~25–30 fC/dot.

Dot size for monolayer exposure decreased with decreasing dose per dot since the beam profile is roughly Gaussian in shape. The minimum dot size was ~5 nm (minimum size) at <7 fC/dot. Figure 3 shows a dot exposed at ~7.6 fC with a cross section that demonstrates that resist resolution is better than ~6 nm. In this figure, the dot is slightly overexposed so the critical resist dimension shown is not through the center of the dot. The edges of the dot (in the fast raster direction) will be at a lower area dose due to the less time the beam spends at the edge of the dot. Below ~4.5 fC/dot, no modifications were observed and the 4.5 fC/dot doses were the same size as the 7 fC/dot doses, but had very little contrast between exposed and unexposed areas in the AFM images. This dose per dot can be compared using the full dot size of ~7 by ~60 nm to get an area dose of ~1.5 mC/cm^2. This is higher than should be required (~100 $\mu C/cm^2$)[6] to expose the ODS layer at this beam energy, but the "full dot size" is somewhat difficult to define because of the elongation in the raster direction. These dots are slightly overexposed, but observing the lower dose dots is very difficult because of the lower contrast in the AFM imaging. Also, the critical dose ~100 $\mu C/cm^2$ corresponds to large area patterns,[6] and the lack of proximity effects in the isolated dots may require a higher effective dose for enough exposure contrast.

At a lower beam energy of 1 keV, the minimum dot size was ~12 nm at 1.3 fC/dot. The backscattering range of electrons should be less at the lower voltage, but the ability to focus the beam is worse and the beam shape is no longer a

Downloaded¬25¬Mar¬2006¬to¬169.237.215.179.¬Redistribution¬subject¬to¬AIP¬license¬or¬copyright,¬see¬http://apl.aip.org/apl/copyright.jsp

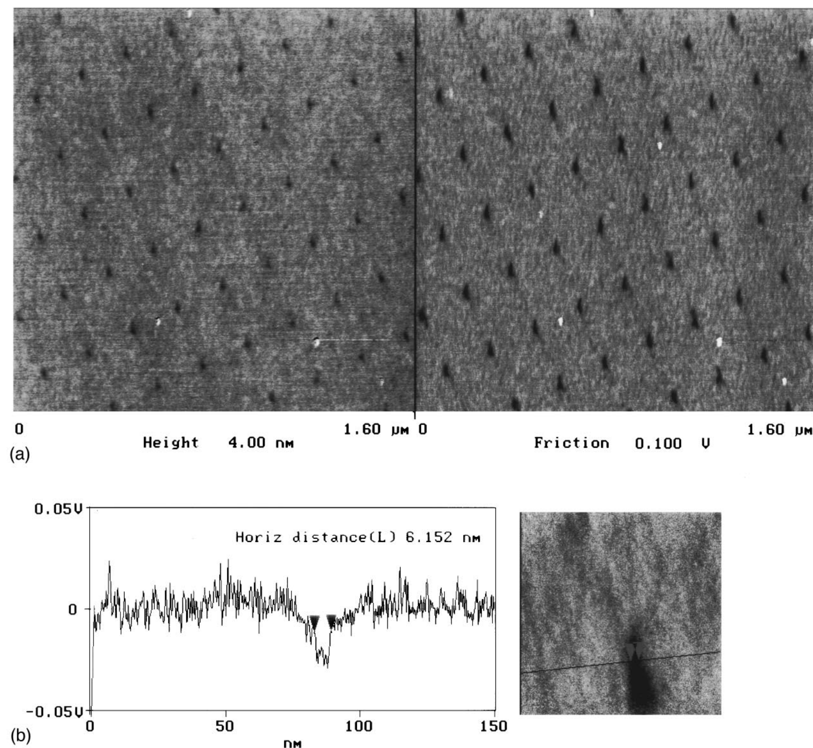

FIG. 3. (a) AFM and FFM image of dots exposed at 20 keV, 7.6 fC/dot. (b) AFM image of single dot from array in (a) along with cross-sectional profile showing a resist resolution ~6 nm. The dot center width is slightly larger because the dot is overexposed.

single Gaussian. Dots were observed at doses down to ~0.47 fC/dot, but these dots were not smaller than those at 1.3 fC/dot, most likely because of the difficulty in focusing at lower beam currents. The approximately 10 times higher sensitivity at lower beam voltage is almost exactly what is predicted from continuous energy loss differences between 1 keV (13.6 eV/nm) and 20 keV (1.2 eV/nm).[14]

Since the measured beam size at 20 keV is smaller than 3 nm, the reason that no dots or critical dimensions below 5 nm were observed should be addressed. Examination of the AFM images shows that there is a noticeable surface roughness in the ODS monolayer. The roughness is very small (~0.15 nm RMS), but coupled with the small contrast in the AFM imaging makes the observation of dots or critical dimensions below 5 nm extremely difficult by this technique. Slightly overexposed dots are easier to find and image; therefore, the critical dimensions at the edges of these dots are used for the resolution measurement. However, the 5 nm limit may also be the resolution limit of these materials because the electron attenuation length in saturated hydrocarbons is fairly steady at ~2.5 nm over the electron energy range 5 to 300 eV,[15] and this energy loss range [from the absorption threshold at 7.2 eV to the C(1*s*) core energy] should account for most electron damage to saturated hydrocarbons.[16] Even a point beam should produce a structure with approximately twice this width. The ultimate molecular limit of these materials is the diameter of the alkyl groups (~0.5 nm), but the range of secondary electrons with enough energy to damage the material will limit the resolution if this range is larger than the molecular size.

Electron beam modification of self-assembled monolayers has been extended to the sub-10 nm regime by using an SEM with a measured small beam diameter. Dots with dimensions of ~5 to 6 nm have been formed at doses of ~7 fC/dot using a 20 keV beam. This provides evidence that self-assembled monolayers may be useful as ultrahigh resolution electron beam resists for the formation of sub-10 structures.

The authors would like to acknowledge funding from the Advanced Research Projects Agency and the use of facilities at the National Nanofabrication Facility (NNF) and facilities at the Cornell Materials Science Center (NSF). M. Lercel would like to acknowledge helpful discussions with M. Rooks (NNF) and D. M. Tannenbaum (Cornell).

[1] A. N. Broers, IBM J. Res. Dev. **32**, 502 (1988).
[2] H. G. Craighead, R. E. Howard, L. D. Jackel, and P. M. Mankiewich, Appl. Phys. Lett. **56**, 2003 (1990).
[3] W. Chen and H. Ahmed, Appl. Phys. Lett. **62**, 1499 (1993).
[4] A. Murray, M. Scheinfein, M. Isaacson, and I. Adesida, J. Vac. Sci. Technol. B **3**, 367 (1985).
[5] A. Ulman, *An Introduction to Ultra-thin Organic Films: Langmuir-Blodgett to Self-Assembly* (Academic, New York, 1991).
[6] M. J. Lercel, R. C. Tiberio, P. F. Chapman, H. G. Craighead, C. W. Sheen, A. N. Parikh, and D. L. Allara, J. Vac. Sci. Technol. B **11**, 2823 (1993).
[7] M. J. Lercel, G. F. Redinbo, H. G. Craighead, C. W. Sheen, and D. L. Allara, Appl. Phys. Lett. **65**, 974 (1994).
[8] M. J. Lercel, M. Rooks, R. C. Tiberio, H. G. Craighead, C. W. Sheen, A. N. Parikh, and D. L. Allara, J. Vac. Sci. Technol. B **13**, 1139 (1995).
[9] Root mean square roughness.
[10] Digital Instruments Inc. (Santa Barbara, CA).
[11] M. Radmacher, R. W. Tillman, M. Fritz, and H. E. Gaub, Science **257**, 1900 (1992).
[12] S. A. Rishton, S. P. Beaumont, and C. D. W. Wilkinson, J. Phys. E **17**, 296 (1984).
[13] "Model 486/487 Picoammeter and Picoammeter/Voltage Source Instruction Manual" (Keithley Instruments, Cleveland, OH).
[14] D. C. Joy and S. Luo, Scanning **11**, 176 (1989).
[15] E. Cartier, P. Pfluger, J. J. Pireaux, and M. Rei Vilar, Appl. Phys. A **44**, 43 (1987).
[16] J. J. Ritsko, J. Chem. Phys. **70**, 5343 (1979).

Downloaded¬25¬Mar¬2006¬to¬169.237.215.179.¬Redistribution¬subject¬to¬AIP¬license¬or¬copyright,¬see¬http://apl.aip.org/apl/copyright.jsp